The Drosophila RZZ complex - roles in membrane trafficking and cytokinesis.

Alan Wainman, Maria Grazia Giansanti, Michael L Goldberg, Maurizio Gatti

The *Drosophila* RZZ complex – roles in membrane trafficking and cytokinesis

Alan Wainman[1,*], Maria Grazia Giansanti[1], Michael L. Goldberg[2] and Maurizio Gatti[1,‡]

[1]Istituto Pasteur-Fondazione Cenci Bolognetti and Istituto di Biologia e Patologia Molecolari (IBPM) del CNR, Dipartimento di Biologia e Biotecnologie, Sapienza, Università di Roma, P. le A. Moro 5, 00185 Roma, Italy
[2]Department of Molecular Biology and Genetics, Biotechnology Building, Cornell University, Università di Roma, NY 14853, Ithaca, USA

*Present address: Sir William Dunn School of Pathology, University of Oxford, South Parks Road, Oxford OX1 3RE, UK
‡Author for correspondence (maurizio.gatti@uniroma1.it)

Accepted 14 May 2012
Journal of Cell Science 125, 4014–4025

doi: 10.1242/jcs.099820

Summary

The Zw10 protein, in the context of the conserved Rod–Zwilch–Zw10 (RZZ) complex, is a kinetochore component required for proper activity of the spindle assembly checkpoint in both *Drosophila* and mammals. In mammalian and yeast cells, the Zw10 homologues, together with the conserved RINT1/Tip20p and NAG/Sec39p proteins, form a second complex involved in vesicle transport between Golgi and ER. However, it is currently unknown whether Zw10 and the NAG family member Rod are also involved in *Drosophila* membrane trafficking. Here we show that Zw10 is enriched at both the Golgi stacks and the ER of *Drosophila* spermatocytes. Rod is concentrated at the Golgi but not at the ER, whereas Zwilch does not accumulate in any membrane compartment. Mutations in *zw10* and RNAi against the *Drosophila* homologue of *RINT1* (*rint1*) cause strong defects in Golgi morphology and reduce the number of Golgi stacks. Mutations in *rod* also affect Golgi morphology, whereas *zwilch* mutants do not exhibit gross Golgi defects. Loss of either Zw10 or Rint1 results in frequent failures of spermatocyte cytokinesis, whereas Rod or Zwilch are not required for this process. Spermatocytes lacking *zw10* or *rint1* function assemble regular central spindles and acto-myosin rings, but furrow ingression halts prematurely due to defective plasma membrane addition. Collectively, our results suggest that Zw10 and Rint1 cooperate in the ER–Golgi trafficking and in plasma membrane formation during spermatocyte cytokinesis. Our findings further suggest that Rod plays a Golgi-related function that is not required for spermatocyte cytokinesis.

Key words: Zw10, Rod, Golgi, ER, cytokinesis, *Drosophila melanogaster*

Introduction

Successful cytokinesis requires the constriction of an acto-myosin ring concurrent with targeted membrane addition at the cleavage furrow (Albertson et al., 2005; Eggert et al., 2006). Membrane formation during cytokinesis depends on components of both the secretory and the endocytic/recycling pathways. In the secretory pathway, vesicles from the ER are transported to the Golgi to be sorted and then shuttled to the plasma membrane. In the endocytic/recycling pathway, plasma membrane-derived vesicles proceed through the early endosome and the recycling endosome, which ultimately directs the vesicles back to the plasma membrane. These pathways involve many factors, including proteins required for vesicle budding and/or coating, for vesicle transport between membrane compartments, and for precise recognition and interactions between the vesicles and the target membrane (reviewed by Albertson et al., 2005; McKay and Burgess, 2011; Montagnac et al., 2008; Prekeris and Gould, 2008). Although membrane addition is crucial for cytokinesis, the inventory of proteins involved in this process is largely incomplete. In addition, it is unclear how the secretory and the endocytic/recycling pathways intersect and cooperate for the proper execution of cytokinesis.

Male meiosis of *Drosophila melanogaster* is a highly suitable system for the identification and functional characterization of membrane-related proteins required for cytokinesis. Spermatocyte cytokinesis depends on a number of proteins involved in the ER–Golgi or intra-Golgi trafficking, including Four Wheel Stop (Fws), the *Drosophila* orthologue of the Cog5 subunit of the conserved oligomeric Golgi complex (Farkas et al., 2003); the conserved Golgi-associated SNARE Syntaxin 5 (Xu et al., 2002); and the TRAPPII subunit encoded by *brunelleschi* (*bru*) (Robinett et al., 2009). Successful spermatocyte cytokinesis also requires the Rab11 and ARF6 GTPases, both of which are enriched at vesicles that mediate membrane addition to the cleavage furrow (Dyer et al., 2007; Giansanti et al., 2007). Other proteins required for spermatocyte cytokinesis in flies are the phosphatidylinositol transfer protein (PITP) encoded by *giotto* (*gio*) (Gatt and Glover, 2006; Giansanti et al., 2006) and the phosphatidylinositol 4-kinase β (PI4Kβ) encoded by *fwd* (Brill et al., 2000; Polevoy et al., 2009). Considered in terms of their global effects on cytokinesis, mutations in *fws*, *bru*, *Rab11*, *Arf6*, *gio* and *fwd* in fact cause very similar defects: Mutant spermatocytes assemble a regular acto-myosin ring but the ring fails to constrict to completion and the furrow regresses, leading to cytokinesis failure. This phenotype is thought to reflect a common defect in membrane addition to the cleavage furrow (Dyer et al., 2007; Gatt and Glover, 2006; Giansanti et al., 2006; Giansanti et al., 2007).

Zw10 is a multifunctional protein that participates both in kinetochore activity and in membrane trafficking. During mitosis, Zw10 forms the RZZ complex with Rough-deal (Rod)

and Zwilch. This evolutionarily conserved complex is a kinetochore component that plays an essential role in the spindle assembly checkpoint (SAC), which blocks the metaphase-to-anaphase transition until all chromosomes are properly aligned in a metaphase plate (Scaërou et al., 2001; Starr et al., 1998; Williams et al., 2003) (reviewed by Karess, 2005; Musacchio and Salmon, 2007). Zw10 homologues are also involved in membrane traffic. In yeast, the Zw10 homologue Dsl1p participates in a single complex that contains the Tip20p and Sec39p proteins. The Dsl1 complex does not function during mitosis, but it is required for the retrograde transport of COP-1 coated vesicles from the Golgi to the ER (Schmitt, 2010).

In mammals, Zw10 forms two complexes: the RZZ complex mentioned above and the NRZ complex. NRZ, the mammalian counterpart of the yeast Dsl1 complex, consists of ZW10 as well as RINT1 (Rad50 Interacting protein 1) and NAG (Neuroblastoma Amplified Gene) that are homologous to yeast Tip20p and Sec39p, respectively. The NRZ complex is enriched at both the Golgi and the ER of mammalian cells and interacts with the ER membrane SNARE proteins Use1p/p31 and BNIP1/Syntaxin-18 (Aoki et al., 2009; Arasaki et al., 2006; Arasaki et al., 2007; Civril et al., 2010; Hirose et al., 2004; Inoue et al., 2008; Varma et al., 2006). However, it is currently unclear whether NRZ mediates the anterograde ER-to-Golgi trafficking, the retrograde Golgi-to-ER trafficking, or both (Aoki et al., 2009; Arasaki et al., 2006; Hirose et al., 2004; Sun et al., 2007). In any event, good agreement exists concerning the importance of NRZ to Golgi maintenance and integrity, because knockdown of either *ZW10* or *RINT1*, but not of *NAG*, results in Golgi fragmentation (Aoki et al., 2009; Arasaki et al., 2006; Hirose et al., 2004; Sun et al., 2007; Varma et al., 2006; Schmitt, 2010). The precise function of ZW10 within the NRZ complex is also unclear. ZW10 might regulate vesicle movement along the microtubules through its interaction with dynein via dynamitin (Varma et al., 2006; Inoue et al., 2008), or it might play a direct role in membrane fusion or budding, or in the maintenance of proper Golgi architecture (Vallee et al., 2006; Sun et al., 2007).

Here we ask whether the components of the *Drosophila* RZZ complex are important for membrane trafficking during spermatogenesis. We show that Zw10 is enriched at the Golgi stacks, the ER, and at the acroblast. Rod is enriched at the Golgi and the acroblast but not at the ER, while Zwilch fails to concentrate in any membrane compartment. We also show that Zw10 and Rod are both required for Golgi integrity and acroblast assembly, while only Zw10 is required for spermatocyte cytokinesis. In addition, we demonstrate that the *Drosophila* homologue of RINT1 (CG8605 or Rint1) is required for Golgi integrity and cytokinesis just like Zw10. Our results suggest roles for Zw10 and Rint1 in ER–Golgi trafficking and membrane addition during cytokinesis; Rod appears to mediate proper Golgi function but is dispensable for cytokinesis. Given their different functions and subcellular localizations, Zw10–Rint1 and Rod might be part of different subcomplexes involved in membrane traffic during *Drosophila* spermatogenesis.

Results

Organization of membrane compartments in *Drosophila* primary spermatocytes

Some familiarity with the ultrastructure of fly spermatocytes is useful to better understand the experiments described below. Mature *Drosophila* spermatocytes (fully grown late prophase primary spermatocytes at stages S5 and S6, according to Cenci et al., 1994) contain multiple Golgi stacks (Fig. 1) that are enriched in the Lava Lamp (Lva) golgin, Fws/Cog5 and the Bru subunit of the TRAPPII complex (Farkas et al., 2003; Fuller, 1993; Giansanti et al., 2006; Giansanti et al., 2007; Robinett et al., 2009; Tates, 1971). At metaphase the Golgi stacks disassemble, giving rise to vesicle-like structures; a fraction of these vesicles fuses with the furrow membrane, contributing to the membrane expansion required for cytokinesis (Farkas et al., 2003; Giansanti et al., 2006; Giansanti et al., 2007).

EM studies showed that in mature spermatocytes the ER cisternae are organized in parallel arrays around the nucleus (Fuller, 1993; Tates, 1971). During prometaphase/metaphase I, the ER undergoes a dramatic morphological transformation. Dividing spermatocytes form the ‘spindle envelope’ (henceforth abbreviated as SE), a structure made of a series of parafusorial membranes that encircle the meiotic chromosomes from

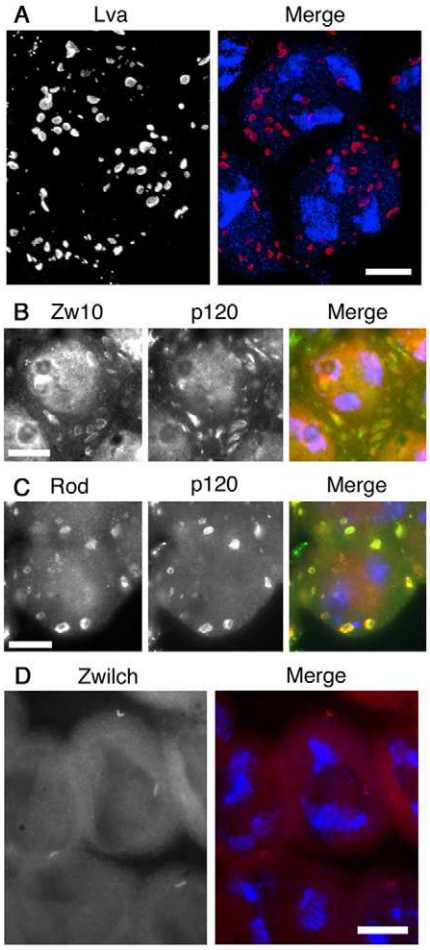

Fig. 1. Zw10 and Rod, but not Zwich, accumulate in the Golgi stacks of mature spermatocytes. (**A–D**) *Drosophila* mature spermatocytes contain multiple Golgi stacks, which are immunostained by anti-Lva (A), anti-Zw10 (B) and anti-Rod (C) antibodies, but not by anti-Zwilch antibodies (D). In merged images, Lva, Zw10, Rod and Zwilch are red, the p120 Golgi protein is green and DNA is blue. The Zw10 and Rod signals are largely coincident with the p120 Golgi signals. Each spermatocyte nucleus contains three distinct DNA clumps that correspond to the three major bivalents (X-Y, 2-2 and 3-3). Centriole staining by the anti-Zwilch antibody is non-specific, as it is also seen in *zwilch* mutants (not shown) (Williams et al., 2003). Scale bars: 10 µm.

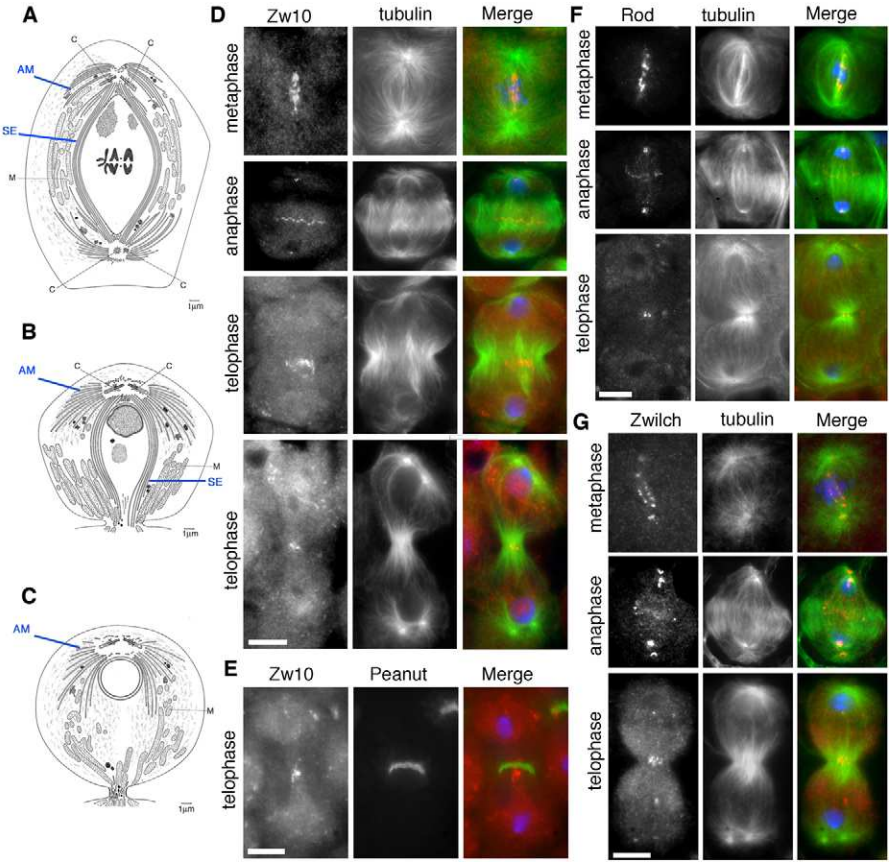

Fig. 2. Subcellular localization of the RZZ complex proteins during the first male meiotic division. (**A–C**) To facilitate understanding of RZZ localization we show diagrams of primary spermatocytes undergoing metaphase (A; entire cell), early telophase (B; half cell) and late telophase (C; half cell). These diagrams are based on electron microscopy studies by A. D. Tates (Tates, 1971) (see also Fuller, 1993) reprinted with permission of the author. Major structures include the centrioles (C), astral membranes (AM), the spindle envelope (SE) consisting of several layers of parafusorial membranes, and mitochondria (M). The spindle MTs, which are not shown in the diagrams, lie both within and outside the SE. (**D**) Zw10 (red in merged images) localizes to the kinetochores and kinetochore MTs during metaphase, and at the SEMZ during ana-telophase; in telophase cells, Zw10 is also enriched at punctae at the cell poles. (**E**) Simultaneous staining for Zw10 (red) and Peanut (green) reveals that the Zw10 signal at the SEMZ is internal to the Peanut signal. (**F**) Rod (red in merges) localization in wild-type primary spermatocytes is comparable to that of Zw10. (**G**) Zwilch (red in merged images) also exhibits a localization pattern comparable to that of Zw10, but fails to concentrate in punctae at the telophase cell poles. The centriole immunostaining is non-specific. In all merged images, tubulin is green and DNA is blue. Scale bars: 10 μm.

metaphase to mid-telophase, eventually disintegrating during late telophase (Fig. 2A–C) (Fuller, 1993; Giansanti et al., 2006; Giansanti et al., 2007; Inoue et al., 2004; Tates, 1971). Dividing spermatocytes also assemble the so-called astral membranes, two prominent membrane networks that overlap with the astral microtubules at the cell poles (Fig. 2A–C). Based on their ultrastructures, it has been suggested that the parafusorial and the astral membranes together constitute the ER of dividing spermatocytes (Fuller, 1993; Tates, 1971). As expected from this idea, spermatocyte structures corresponding to the spindle envelope and the astral membranes are in fact enriched in the ER marker Protein disulfide isomerase (Pdi) fused with GFP (Bobinnec et al., 2003; Giansanti et al., 2006; Giansanti et al., 2007).

Zw10, Rod and Zwilch localization in primary spermatocytes

Earlier studies showed that during metaphase Zw10 accumulates at kinetochores, colocalizing with Rod and Zwilch. If the chromosomes are properly connected to kinetochore microtubules (MTs) in a bipolar fashion, the three proteins of the RZZ complex stream off the kinetochores by moving along kinetochore MTs toward the spindle poles (Fig. 2) (Scaërou et al., 2001; Williams et al., 1992; Williams et al., 1996). Zw10 has also previously been found to be enriched at the midbody of telophase spindles, while Rod and Zwilch did not appear to concentrate in this structure (Scaërou et al., 2001; Williams et al., 1996; Williams et al., 2003).

In light of the recently described role for Zw10 in ER–Golgi trafficking, we decided to re-examine the localization of the three RZZ proteins in *Drosophila* spermatocytes. In wild-type mature spermatocytes, Zw10 and Rod localized to discrete structures resembling the Golgi stacks prior to their dispersal during prometaphase (Fig. 1B,C). These structures were unambiguously recognized as Golgi stacks because they reacted with the p120 monoclonal antibody directed against an integral Golgi membrane protein (Stanley et al., 1997) (Fig. 1B,C). In contrast, Zwilch localized diffusely within the cytoplasm of mature spermatocytes and did not concentrate in the Golgi stacks (Fig. 1D). During anaphase and telophase I, Zw10 was enriched in broad areas at the cell poles and often concentrated in small structures located in the same areas (Fig. 2D,E). These structures are reminiscent of the Golgi-derived vesicles detected by Lva or Rab11 staining, but appear smaller than them (compare Fig. 2D with Fig. 5 below) (see also Giansanti et al., 2007). Faintly stained vesicle-like structures were also observed at the poles of ana-telophase I spermatocytes immunostained for Rod (Fig. 2F) but not for Zwilch (Fig. 2G). Interestingly, all three RZZ components were enriched within the SE and aggregated to form a band at the SE midzone (SEMZ; Fig. 2D–G). The accumulation of Zw10, Rod and Zwilch at the SEMZ becomes more pronounced with the progression of telophase I; in late telophases, these proteins appear as compact aggregates located at the interior of the equatorial region of the cell (Fig. 2D–G). To demonstrate that the Zw10, Rod and Zwilch accumulations at the SEMZ do not correspond to the contractile rings, we co-stained telophase I spermatocytes for Zw10 and Peanut, one of the *Drosophila* septins associated with the contractile ring (Neufeld and Rubin, 1994). We observed two spatially distinct structures at the equatorial site, with the Zw10 aggregate interior to the Peanut ring (Fig. 2E).

Zw10 and Rod are required for Golgi stack integrity

In mammalian cells, depletion of either ZW10 or RINT1, but not of NAG, results in Golgi fragmentation, suggesting a role for ZW10 and RINT1 in maintaining Golgi integrity (Aoki et al., 2009; Arasaki et al., 2006; Hirose et al., 2004; Sun et al., 2007; Varma et al., 2006). We thus asked whether the RZZ proteins are necessary for Golgi stack integrity in mature spermatocytes. Staining for the Golgi marker Lva showed that mature wild-type spermatocytes contain approximately 20 Golgi stacks per cell; most of these stacks have a bi-concave disc shape (Fig. 3A,E,F). In *zw10* mutant spermatocytes, the Golgi structures were less numerous (~10/cell) than in wild type and exhibited severe morphological defects (Fig. 3B,E,F). In spermatocytes from *rod* mutants, the number of Golgi structures was normal but their morphology was highly irregular (Fig. 3C,E,F). The Golgi structures observed in *zwilch* mutant spermatocytes appeared normal in number but showed a mild defect in shape (Fig. 3D–F).

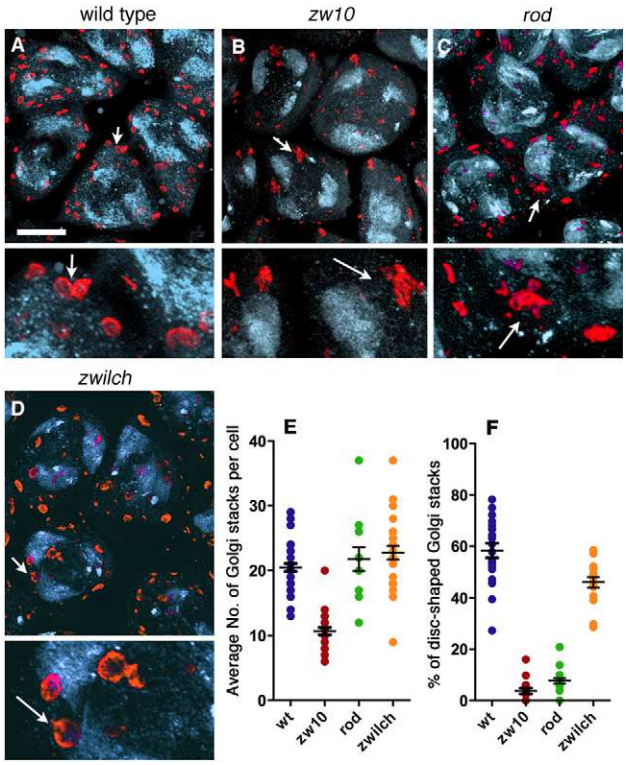

Fig. 3. Mutations in *zw10* and *rod* affect Golgi stack number and/or morphology, whereas mutations in *zwilch* do not cause Golgi defects. (**A–D**) Mature spermatocytes from wild-type (A), *zw10* (B), *rod* (C) and *zwilch* (D) mutant larvae stained for Lva (Red) and DNA (blue). Enlarged areas below each panel (arrows mark identical sites) show the detailed morphology of the Golgi stacks. Scale bar: 10 µm. (**E**) Average number of Golgi stacks per cell (± s.e.m.). (**F**) Frequencies of Golgi stacks with a normal disc-shaped morphology (± s.e.m.). These frequencies were determined by 'blind' examination of enlarged microphotographs; each point in the graph (20 for wild type; 15 for *zw10*, 17 for *rod* and 17 for *zwilch*) corresponds to either a single spermatocyte or a group of two or three spermatocytes. In *zw10* mutants, the number and morphology of Golgi stacks are severely affected (B,E,F); most Golgi structures are smaller than in wild type or consist of multiple collapsed Golgi stacks (arrows in B). In *rod* mutants, the number of Golgi structures is normal but their morphology is affected (C,E,F). Mutations in *zwilch* do not affect the number of Golgi stacks and do not cause gross defects in Golgi morphology (D,E,F).

We believe that this minor defect is not a direct effect of *zwilch* knockdown, but is rather a consequence of Zwilch depletion affecting the other RZZ components (see below). These observations demonstrate that Zw10 and Rod play membrane trafficking functions crucial for Golgi structural integrity in *Drosophila* spermatocytes.

Dynein does not co-localize with Zw10 in *Drosophila* spermatocytes

It has been proposed that the interaction of Zw10 with the dynein motor complex facilitates retrograde vesicle movement (Varma et al., 2006), although this idea remains controversial (Sun et al., 2007). To investigate whether the dynein complex is involved in Golgi–ER function in *Drosophila*, we examined the localization in wild-type spermatocytes of the dynein light intermediate chain fused with GFP (Dlic–GFP). We found that Dlic–GFP was diffuse in the cytoplasm and concentrated around the centrosomes and at the nuclear envelope. However, in contrast with Zw10, it was not enriched at the Golgi stacks of mature spermatocytes or at the ER during meiosis (supplementary material Fig. S1, Movie 1; data not shown).

Zw10 is the only RZZ component required for spermatocyte cytokinesis

Meiosis in wild-type males produces 64 spermatids, each containing a nucleus and a mitochondrial derivative called the nebenkern (Fuller, 1993). Failure of cytokinesis abrogates proper mitochondria partitioning between the daughter cells, resulting in spermatids composed of an abnormally large nebenkern associated with two or four nuclei of regular size (Fuller, 1993). Errors in chromosome segregation result in spermatid nuclei of different sizes (González et al., 1989).

Previous studies showed that *zw10* mutants exhibit spermatids with a single large nebenkern associated with multiple nuclei of different sizes, indicating defects in both chromosome segregation and cytokinesis (Williams et al., 1996). However, a detailed characterization of the roles of the RZZ components in spermatocyte cytokinesis has not yet been performed. We thus examined spermatid morphology in *zw10*, *rod* and *zwilch* mutants. We also analyzed mutants in *nudE* and *cenp-meta* (*cmet*; one of the two homologues of mammalian *CENPE*), because the protein products of both genes physically interact with Zw10, are involved in the SAC machinery, and accumulate at the SEMZ (Williams et al., 2003; Wainman et al., 2009). The analysis of live spermatids from testis squashes of third instar larvae confirmed the presence of multinucleated spermatids with a single large nebenkern in *zw10* mutants, but did not reveal similar cytokinesis defects in *rod*, *zwilch*, *cmet* or *nudE* mutants (Table 1).

The *Drosophila* homologue of *RINT1* is required for Golgi integrity and cytokinesis

Because the RINT1 component of the mammalian NRZ complex is required for Golgi integrity (Arasaki et al., 2006; Sun et al., 2007), we decided to examine the role of the gene encoding the *Drosophila* homologue of *RINT1* (*CG8605*; henceforth designated as *rint1*) in the maintenance of Golgi structure and cytokinesis. Because there are no extant mutants in *rint1*, we knocked down the gene in testes using an anti-*rint1* UAS–RNAi construct driven by a testis-specific *bam-GAL4* driver (Chen and McKearin, 2003). Staining for Lva showed that spermatocytes

Table 1. Frequencies of multinucleate spermatids in *zw10*, *rod*, *zwilch*, *nudE* and *cenp-meta* mutants, and in *rint1* RNAi testes

Genotype	Number of spermatids	Number of spermatids (nuclei:nebenkern)				% Abnormal
		1:1	2:1	3:1	4:1	
wild-type	500	498	2	0	0	0.4
$zw10^{65i21}$	1619	963	541	4	111	40.5
$zw10^{65i20}$	543	194	293	0	56	64.3
$zwilch^{1229}$	1097	1075	22	0	0	2.0
rod^{1100}	1068	1054	14	0	0	1.3
$nudE^{39E}$	659	655	4	0	0	0.6
$cenp\text{-}meta^{A}$	274	270	4	0	0	1.5
Rint1 RNAi	450	156	102	0	192	65.3

bearing both the RNAi construct and the driver exhibit a substantial reduction in Golgi number (~10/cell) and strong defects in Golgi morphology; spermatocytes carrying either the RNAi construct alone or the driver alone contained normal numbers of Golgi stacks (~20/cell) and did not show Golgi defects (Fig. 4A–C). We note that the pattern of Golgi defects displayed by *rint1* RNAi spermatocytes is very similar to that shown by *zw10* mutant spermatocytes (compare the data in Figs 3 and 4).

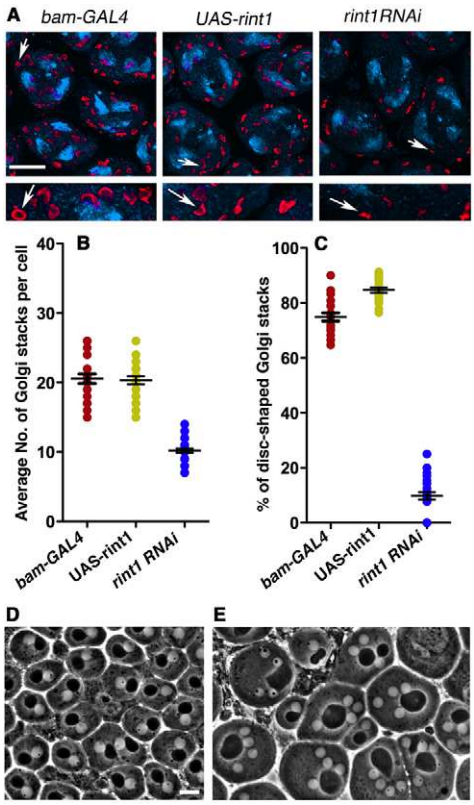

Fig. 4. RNAi-mediated knock down of *rint1* affects Golgi number and morphology and disrupts cytokinesis. (**A**) Mature spermatocytes carrying the *bam-GAL4* driver alone, the *UAS-rint1* RNAi construct (*UAS-rint1*) alone, or both *UAS-rint1* and *bam-GAL4* (*rint1* RNAi), stained for Lva (Red) and DNA (blue). The enlarged areas below each panel (arrows mark identical sites) show the detailed Golgi morphology. Scale bar: 10 μm. (**B**) Average number of Golgi stacks per cell (± s.e.m.). (**C**) Frequencies of Golgi stacks with a normal disc-shaped morphology (± s.e.m.). These frequencies were determined as described in the legend of Fig. 3; each point in the graph (20 for *bam-GAL4*; 22 for *UAS-rint1* and 34 *rint1* RNAi) corresponds to a single spermatocyte. (**D**,**E**) Live spermatid morphology in wild-type (D) and *rint1* RNAi (E) flies. Nuclei are phase-light and the neberken mitochondrial derivatives phase-dense. Scale bars: 10 μm.

Analysis of live testes from *rint1* RNAi flies revealed the presence of many multinucleate spermatids (Table 1; Fig. 4D). However, whereas the spermatid nuclei observed in *zw10* mutants vary in size (Williams et al., 1996) (and confirmed here), those of *rint1* RNAi spermatids are all of the same size. Thus, while Zw10 is required for both meiotic chromosome segregation and cytokinesis, Rint1 is only required for cytokinesis.

Failure in RZZ assembly at the kinetochore redistributes Zw10 and Rod to diverse membrane compartments

Because the RZZ complex fails to assemble and localize to the kinetochores in the absence of any of its component subunits (Scaërou et al., 2001; Williams et al., 2003), we asked whether failure in RZZ assembly affects Zw10, Rod or Zwilch localization patterns with respect to the membranous structures of spermatocytes. We thus examined Zw10 localization in *rod* and *zwilch* mutants, Rod localization in *zwilch* and *zw10* mutants, and Zwilch localization in *rod* and *zw10* mutants. The analysis of *rod* and *zwilch* mutant spermatocytes revealed a striking relocalization of the Zw10 protein. In both mutants, Zw10 was enriched at the Golgi stacks of mature premeiotic spermatocytes as in wild type (data not shown), but then failed to associate with the kinetochores during metaphase, as expected from previous results (Fig. 5A,B) (see also Williams et al., 2003). However, during meiotic divisions of *rod* and *zwilch* mutant spermatocytes, Zw10 no longer accumulated at the SEMZ, and was instead highly enriched at the SE itself and at the astral membrane region (Fig. 5A,B). This localization was similar to that exhibited by the ER markers GFP–Pdi (Bobinnec et al., 2003; Giansanti et al., 2006; Giansanti et al., 2007) and ER–YFP (LaJeunesse et al., 2004) (see supplementary material Fig. S2). The Zw10 relocalization pattern is also reminiscent of Rab11 localization. However, while Rab11 is enriched at vesicle-like structures at the cell poles and concentrates at the cleavage site (Giansanti et al., 2007), Zw10 decorates only small punctae at cell poles and fails to accumulate at the cleavage furrow.

In mature spermatocytes of *zwilch* and *zw10* mutants, Rod was normally enriched at the Golgi stacks (supplementary material Fig. S3 and data not shown). However, in dividing spermatocytes of both mutants Rod behaved very differently from Zw10. Rod failed to concentrate at the SEMZ just like Zw10, but in contrast with Zw10, it did not accumulate at the SE or at the astral membrane region (Fig. 5C). Instead, in metaphase I cells, Rod was enriched at relatively large structures that we interpret to be remnants of the Golgi stacks that failed to disintegrate (as would

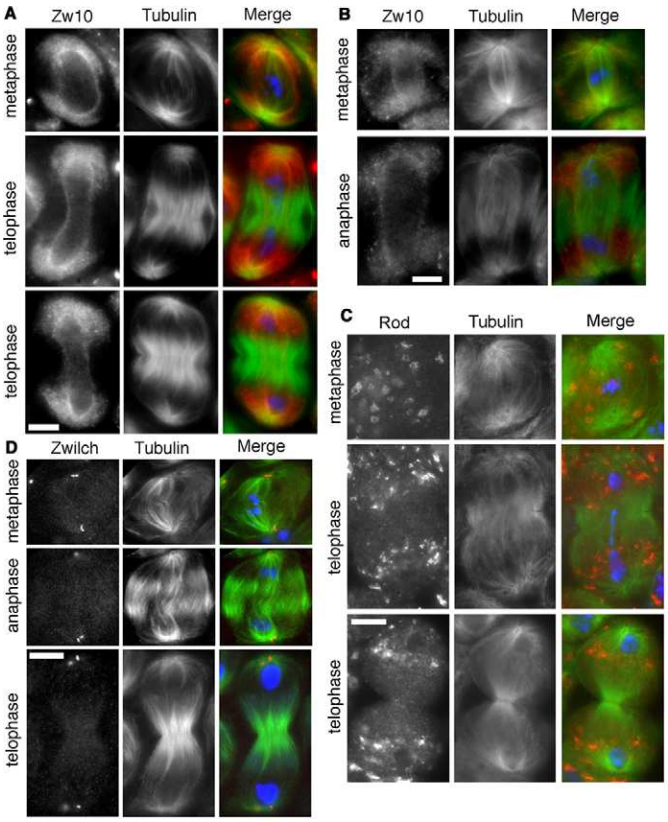

Fig. 5. Failure to assemble an RZZ complex results in redistribution of its components. (**A**) Zw10 localization in dividing primary spermatocytes from *zwilch* mutant larvae. Zw10 fails to associate with kinetochores; it accumulates at the SE and at the cell poles but not at the SEMZ. (**B**) Zw10 localization in *rod* mutant primary spermatocytes is very similar to that observed in *zwilch* mutants (compare with A). (**C**) In both metaphases and ana-telophases of *zwilch* mutant spermatocytes, Rod localizes to multiple structures that are probably Golgi stacks and/or Golgi fragments (see text for further explanation), but fails to accumulate at the SE and the SEMZ. (**D**) In *rod* mutant primary spermatocytes, Zwilch is diffuse in the cytoplasm and does not decorate specific structures (centriole staining is non-specific). In all merged images, Zw10, Zwilch or Rod are red, MTs are green and DNA is blue. Scale bars: 10 μm.

be normal) in preparation for meiosis (Fig. 5C; supplementary material Fig. S3). These structures were never seen in wild-type metaphase I spermatocytes stained for Rod, nor in *zwilch* mutant spermatocytes stained for Zw10 or Lva. *zwilch* and *zw10* mutant ana-telophases I displayed Rod-stained structures at the cell poles (Fig. 5C; supplementary material Fig. S3) that are reminiscent of, but larger than, the Lva positive Golgi remnants seen in wild-type ana-telophases (Giansanti et al., 2006; Giansanti et al., 2007) (see also Fig. 6E below). In *rod* and *zw10* mutant spermatocytes, Zwilch neither exhibited its typical wild-type localization pattern nor showed the types of redistribution observed for Zw10 or Rod; instead it displayed a diffuse localization (Fig. 5D, and data not shown).

We also examined Rod and Zw10 localization in *rint1* RNAi spermatocytes. While Rod was normally enriched at the defective Golgi stacks of *rint1* RNAi mature spermatocytes, Zw10 failed to associate with these structures (supplementary material Fig. S3A,B). The two proteins were both associated with the kinetochores and the spindle MTs during metaphase (supplementary material Fig. S3D), consistent with the finding that Rint1 depletion does not disrupt chromosome segregation (see Fig. 4E). Meiotic ana-telophases of *rint1* RNAi males displayed distributions of the Zw10 and Rod proteins comparable to those seen in wild type, suggesting that these proteins redistribute to membranous structures only when they fail to associate with kinetochores and spindle MTs (not shown).

Collectively, these results suggest that failure to form the RZZ complex increases the amounts of Zw10 and Rod available for membrane trafficking, leading to increases in the concentrations of these proteins in membrane compartments. During meiosis, Zw10 redistributed to both the ER (SE and astral membranes) and small Golgi fragments. In contrast, Rod failed to associate with the ER and only decorated structures that appear to be abnormally large Golgi remnants. An increase in the available amount of Zwilch in *rod* and *zw10* mutants did not cause an obvious accumulation of Zwilch in any membrane compartment, further suggesting that Zwilch is not involved in membrane trafficking.

These findings prompted us to ask whether Zw10 is required for proper formation of the ER of dividing spermatocytes. To assess the effects of *zw10* mutations on the ER we used ER–YFP, which contains both the ER targeting sequence of Calreticulin and the KDEL ER retention signal (LaJeunesse et al., 2004). In *zw10* mutants expressing ER–YFP, the SE and the astral membrane structures were similar to those of wild type from metaphase to late anaphase (supplementary material Fig. S2, Movies 2,3). However, during telophase, the SE of the mutant was often unconstricted at its equator (supplementary material Fig. S2, Movie 3) due to furrow ingression failure (see below). Thus, we conclude that the overall structure of the ER is not grossly affected by *zw10* mutations, except very late in meiosis as a secondary consequence of incomplete cytokinesis.

Zw10 is required for complete furrow ingression

During telophase *Drosophila* spermatocytes exhibit two major cytokinetic structures: the contractile ring that contains proteins such as actin, myosin, anillin and the septins and is located just beneath the plasma membrane (reviewed by D'Avino, 2009); and the central spindle, a prominent bundle of MTs between the two daughter nuclei, that accumulates at its midzone several MT-binding proteins including the Pavarotti kinesin and Fascetto/PRC1 (reviewed by D'Avino et al., 2005). To determine the primary defect leading to cytokinesis failure in *zw10* mutants, we first analyzed fixed cells for the presence and the normality of both the contractile ring and the central spindle. *zw10* mutant spermatocytes displayed clear actin rings during late anaphase (86% normal, $n=29$), but these rings failed to constrict during mid-telophase and appeared fragmented by late telophase (85% defective, $n=20$; supplementary material Fig S4A). Similarly, normal anillin or Peanut rings formed in *zw10* mutant spermatocytes during late anaphase just as in wild type, but by late telophase 60% ($n=20$) of the anillin rings and 65% ($n=20$) of the Peanut rings appeared only poorly constricted (Fig. 6A; supplementary material Fig. S4B). To analyze the central spindle, we immunostained spermatocytes for both tubulin and Fascetto (Feo), a PRC1 homologue that binds the MTs of the central spindle midzone (Vernì et al., 2004). We found that the central spindle was regular during anaphase and early telophase in *zw10* mutants (Fig. 6B), but in 64% of late telophases ($n=40$) the

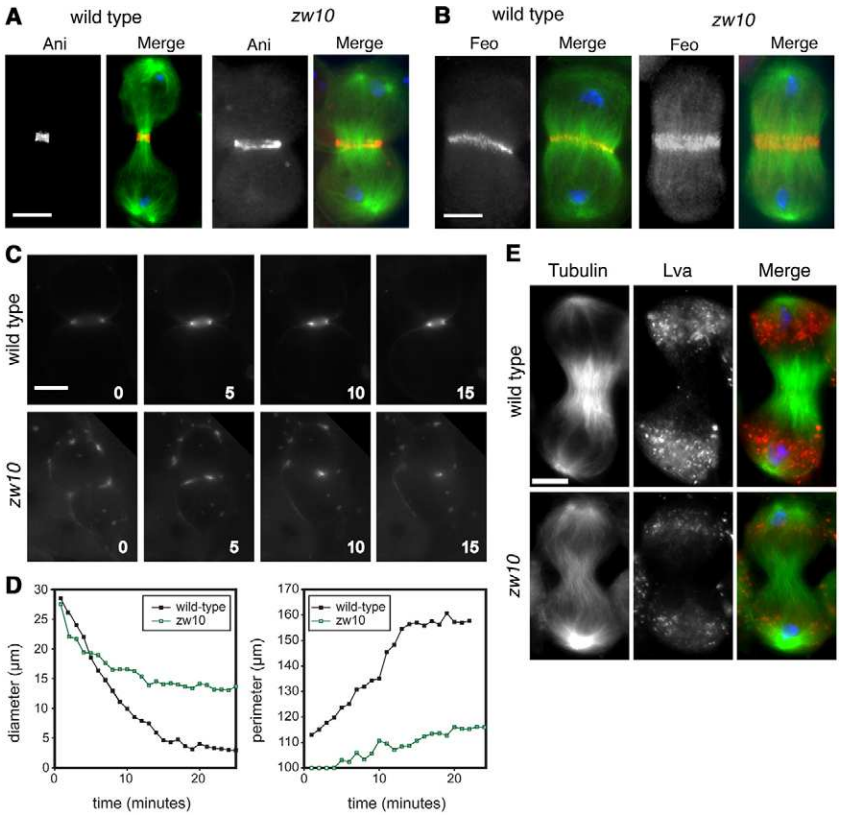

Fig. 6. Incomplete furrow ingression in *zw10* mutants is the result of reduced membrane addition. (**A**) Wild-type and *zw10* mutant spermatocytes in late telophase (as characterized by the first indications of aster separation at the cell poles) exhibit strikingly different degrees of anillin ring constriction (anillin, red; tubulin, green; DNA, blue). (**B**) Wild-type and *zw10* primary spermatocytes in late anaphase/early telophase have comparable central spindles and Feo/PRC1 signals (Feo, red; tubulin, green; DNA, blue). (**C**) Still images from supplementary material Movies 5 and 6 showing dividing primary spermatocytes from wild-type and *zw10* mutant larvae expressing Sqh–GFP (numbers are time, in minutes, following furrow initiation). (**D**) Furrow ingression dynamics in representative wild-type and *zw10* primary spermatocytes showing variations with time (minutes following furrow ingression initiation) of the equatorial diameter and perimeter. (**E**) Staining of late telophase spermatocytes for Lva (red), tubulin (green) and DNA (blue) shows that Golgi-derived vesicles are excluded from the cell equator in both wild-type and *zw10* mutant cells. Scale bars: 10 μm.

structure appeared less dense than in wild type and was irregularly shaped (not shown).

We confirmed these observations by in vivo analysis. Imaging of living spermatocytes expressing GFP–tubulin showed that the central spindle forms regularly in all wild-type and *zw10* mutant cells (supplementary material Fig. S5, Movies 4,5). However, in all mutant cells (n=6) in which the furrow started to ingress but then halted ingression, the central spindle eventually degenerated (supplementary material Fig. S5, Movie 5). Live imaging of spermatocytes expressing a GFP-tagged myosin-regulatory light chain (Sqh–GFP) as a marker for the contractile ring revealed that *zw10* mutants assemble normal contractile rings during anaphase. However, furrow ingression was only partial in 60% of the cells (n=10), and the furrow eventually regressed concurrent with a loss of Sqh–GFP ring integrity (Fig. 6C; supplementary material Movies 6,7).

The cell perimeter increase observed during cytokinesis correlates with an increase in the total surface area, providing a measure of membrane addition (Dyer et al., 2007). Importantly, the increase of membrane surface is not related to the extent of furrow ingression, as mutants where ingression is suppressed due to a failure in contractile ring assembly display a rate of membrane addition comparable to wild type (Dyer et al., 2007). We measured the cell perimeter increase in 5 *zw10* mutant primary spermatocytes defective in furrow ingression. In all cases the perimeter increase was substantially lower than in wild-type spermatocytes (Fig. 6D; supplementary material Fig. S4C). As a representative example of our analysis, Fig. 6D shows that in the mutant spermatocyte the cell diameter at the furrow site fails to decrease compared to wild type, while the perimeter of the same cells fails to increase at the wild-type rate. We note that the low rate of perimeter increase observed in meiotic cells of *zw10* mutants (Fig. 6D; supplementary material Fig. S4C) is comparable to that previously observed in *Arf6* mutant spermatocytes (Dyer et al., 2007). Thus, we conclude that in *zw10* mutant spermatocytes not only is the furrow unable to ingress completely, but also the addition of new membrane during cytokinesis is severely compromised.

We next asked whether *zw10* is required for the fusion of Golgi-derived vesicles with the furrow membrane; this fusion fails to occur in *gio*, *fwd* and *Rab11* mutant spermatocytes, leading to the accumulation of Lva-stained vesicles in the proximity of the cleavage site (Giansanti et al., 2006; Giansanti et al., 2007). In *zw10* spermatocytes, Lva-stained vesicles failed to accumulate near the cleavage furrow and instead remained in the region that surrounds the dividing nuclei in a pattern similar to wild type (Fig. 6E). This result suggests that Zw10 is not required vesicle fusion with the equatorial membrane, just as *fws* and *bru*.

We also examined meiotic ana-telophases in *rint1* RNAi testes. They displayed a phenotype fully comparable to that observed in *zw10* mutants. The central spindle and the contractile ring were both regular during anaphase and early telophase, but the contractile ring failed to constrict properly in most telophases and the central spindle eventually degenerated (of the 30 late telophases examined, 53% displayed an unconstricted anillin ring and 33% a defective central spindle; supplementary material Fig. S4D). In addition, *rint1* RNAi telophases did not accumulate Lva-stained vesicles near the cleavage furrow (supplementary material Fig. S4E).

Roles of Zw10 and Rod in acroblast formation

The *Drosophila* acroblast is a membranous structure situated at the anterior side of the nuclei of elongating spermatids (Fuller 1993; Tates 1971; Wilson et al., 2006). Previous studies showed that the *Drosophila* acroblast forms after the spermatid onion stage from Golgi-derived vesicles; the acroblast is enriched in the

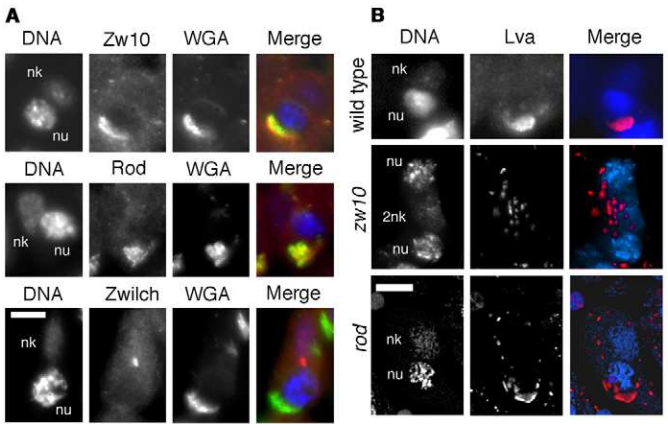

Fig. 7. Zw10 and Rod, but not Zwilch, are enriched at the acroblast and are required for acroblast formation. (**A**) Wild-type spermatids stained for Zw10, Rod or Zwilch (red in merged images), DNA (DAPI; blue), and fluorescein-conjugated wheat germ agglutinin (WGA; green), which marks the acroblast. The Zw10 and Rod signals largely overlap WGA staining in merged images. In contrast, Zwilch is not enriched in the WGA-stained acroblast (the basal body staining is non-specific). nu, nuclei; nk, nebenkern. The nebenkern are weakly fluorescent after DAPI staining because of mitochondrial DNA. (**B**) Wild-type, *zw10* and *rod* mutant spermatids stained for Lva (red) and DNA (blue). Note that the nuclei of *zw10* mutant spermatids are associated with many Golgi vesicles but lack an organized acroblast; 2nk indicates a double-sized nebenkern resulting from cytokinesis failure. In the *rod* mutant spermatid, the acroblast is only partially assembled; the cell exhibits a small acroblast associated with several unfused vesicles. Scale bars: 10 μm.

Lva, Fws, Rab11 and Bru proteins and is stained by fluorescein-conjugated wheat germ agglutinin (WGA) (Farkas et al., 2003; Giansanti et al., 2006; Giansanti et al., 2007; Robinett et al., 2009). We found that Zw10 and Rod localize to a conical structure at the anterior side of spermatid nuclei resembling the acroblast in both location and morphology (Fig. 7A). The Zw10 and Rod signals coincided with WGA staining, indicating that the Zw10- and Rod-enriched structures in spermatids are indeed the acroblasts (Fig. 7A). Immunostaining for Zwilch did not reveal any spermatid-associated structure, indicating that the acroblast is not enriched in the Zwilch protein (Fig. 7A).

We next asked whether Zw10 and Rod are required for acroblast formation. In wild-type spermatids stained for Lva, the acroblast appears as a continuous structure (Fig. 7B) (Farkas et al., 2003), whereas in *zw10* spermatids the acroblast consistently appeared as an aggregate of multiple unfused vesicles (Fig. 7B). In rod mutants, approximately one half the acroblasts consisted of unfused vesicles, while the other half were apparently normal (Fig. 7B). Thus, we conclude that Zw10 and Rod are not only enriched at the acroblast but are also required for the assembly of this structure.

Discussion

Zw10 was initially identified through its role in *Drosophila* chromosome segregation (Smith et al., 1985; Williams et al., 1992; Williams et al., 1996; Williams and Goldberg, 1994), and was subsequently shown to be part of the conserved RZZ complex required for proper SAC functioning in both *Drosophila* and mammals (Scaërou et al., 2001; Williams et al., 2003) (reviewed by Karess, 2005; Musacchio and Salmon, 2007). Recent work has shown that the Zw10 homologues of mammals (ZW10) and yeast (Dsl1) interact with the conserved RINT-1/Tip20p and NAG/Sec39p proteins, forming a different complex that is required for membrane traffic between the ER and the Golgi (Arasaki et al., 2006; Civril et al., 2010; Hirose et al., 2004; Inoue et al., 2008; Schmitt, 2010; Sun et al., 2007). Moreover, it has been suggested that mammalian NAG and ROD are structurally and phylogenetically related proteins (Civril et al., 2010), yet the *Drosophila* genome has only a clear ROD homologue but no NAG homologue. Does *Drosophila* Zw10 then participate in membrane trafficking, and if so, is this role performed in conjunction with Rod, which in mammalian cells appears to function only at the kinetochore? The highly patterned structure of *Drosophila* spermatocytes allowed us to examine these questions in detail by determining whether any of the RZZ proteins are necessary for any of the specialized membranous structures easily recognized in these cells.

Roles of ZW10, Rod and Rint1 in *Drosophila* membrane trafficking

Our cytological and phenotypic analyses demonstrate for the first time that Zw10 plays a role in *Drosophila* membrane traffic. During male meiosis Zw10 is enriched both at the Golgi stacks and at ER structures such as the spindle envelope and the astral membranes. In addition, we determined that Zw10 localizes to the spermatid acroblast, which assembles from Golgi-derived vesicles (Farkas et al., 2003; Giansanti et al., 2006; Giansanti et al., 2007) and exhibits an ultrastructure reminiscent of the Golgi ribbons of mammalian cells (Kondylis and Rabouille, 2009). ZW10 enrichment at both the Golgi and the ER has been also observed in mammalian cells (Arasaki et al., 2006; Arasaki et al., 2007; Civril et al., 2010; Hirose et al., 2004; Inoue et al., 2008; Varma et al., 2006). Consistent with these findings, *Drosophila* spermatocytes and mammalian tissue culture cells both exhibit Golgi fragmentation following Zw10 depletion (this report) (Hirose et al., 2004; Sun et al., 2007; Varma et al., 2006). These phenotypic similarities strongly suggest that *Drosophila* Zw10 and its mammalian counterpart play comparable roles in ER–Golgi trafficking.

We do not know whether *Drosophila* Zw10 specifically mediates anterograde (Hirose et al., 2004) or retrograde (Aoki et al., 2009; Arasaki et al., 2006; Sun et al., 2007) transport between the ER and Golgi, or instead influences traffic in both directions (Aoki et al., 2009; Arasaki et al., 2006). Nor do we know whether *Drosophila* Zw10 forms a complex comparable to the conserved NRZ/Dsl1 complex (NAG/Sec39p–RINT1/Tip20p–ZW10/Dsl1p). However we found that RNAi against the *Drosophila* homologue of RINT1/Tip20p (CG8605, FlyBase) (Schmitt, 2010) causes Golgi defects that are indistinguishable from those observed in *zw10* mutant spermatocytes. Consistent with these results, previous studies have shown that human cells exhibit nearly identical Golgi defects after depletion of either ZW10 or RINT1 (Sun et al., 2007). In addition, we found that Rint1 is required for Zw10 but not for Rod localization to the Golgi stacks of mature spermatocytes, and that loss of either Zw10 or Rint1 results in comparable cytokinetic defects. Thus, Zw10 or Rint1 depletion result in comparable phenotypes, and Zw10 localization to the Golgi depends on Rint1, suggesting that these proteins might form a complex like their mammalian counterparts.

Our results indicate that also Rod performs a function in membrane traffic in *Drosophila* testes. Like Zw10, Rod is enriched at both the Golgi stacks and the acroblast of wild-type males and is required for the formation and/or integrity of both structures. However, Rod and Zw10 display very different redistribution patterns in *zwilch* mutants. We presume that failure to form the RZZ complex would increase the amounts of Zw10 and Rod available for membrane trafficking, leading to increases in the concentrations of these proteins in those membrane compartments in which they are normally found. Under this interpretation, our results emphasize that Zw10 is enriched at both the Golgi and the ER, whereas Rod appears to localize only at the Golgi. Less clear is the nature of the Rod-enriched structures seen in metaphase and ana-telophase of *zwilch* and *zw10* mutants. We propose that Rod 'overexpression' in *zwilch* and *zw10* mutants affects disassembly of the Golgi stacks at metaphase, leading to the formation of abnormally large Golgi fragments, which persist during ana-telophase. These aberrant Golgi-derived structures retain Rod but lose Zw10 and Lva, both of which are present earlier in the Golgi stacks of premeiotic spermatocytes. Due to the current lack of suitable antibodies against *Drosophila* Golgi components (see Materials and Methods), we could not determine whether these Rod-containing structures are also enriched in other known Golgi proteins.

The finding that Rod plays a role in membrane traffic at the Golgi has important evolutionary implications. As mentioned earlier, mammalian ROD and NAG are structurally related, suggesting that they evolved from a common ancestor involved in membrane trafficking (Civril et al., 2010). Since BLAST searches do not reveal Rod paralogs in the fly genome, *Drosophila* Rod could correspond to the hypothesized ancestor of ROD and NAG. Alternatively, *Drosophila* may have lost its NAG homologue during evolution (Schmitt, 2010), and Rod acquired certain NAG functions. Both ideas are consistent with our results that *Drosophila* Rod has a dual role, functioning in both the spindle assembly checkpoint and membrane trafficking. The precise membrane-related function of Rod is currently unclear, but it appears to be separated from those of Zw10 and Rint1. We propose that Zw10–Rint1 and Rod participate in different subcomplexes affecting different aspects of membrane traffic during *Drosophila* spermatogenesis.

The roles of Zw10 and Rint1 in spermatocyte cytokinesis

We have shown that *zw10* mutant and *rint1* RNAi spermatocytes exhibit very similar defects in cytokinesis. Both assemble regular central spindles and acto-myosin rings. However, in most Zw10 or Rint1-depleted spermatocytes, furrow ingression halts prematurely and the furrow eventually regresses, leading to a failure of cytokinesis. Concomitant with furrow regression, the central spindle progressively disassembles, consistent with the known interdependence between the central spindle and the contractile ring (Giansanti et al., 1998). This abortive cytokinesis phenotype is similar to that displayed by mutants in *gio* (PITP), *fwd* (PI4Kβ), *Rab11*, *fws* (Cog5), *bru* (TRAPPII) and *Arf6* (Brill et al., 2000; Dyer et al., 2007; Gatt and Glover, 2006; Giansanti et al., 2004; Giansanti et al., 2006; Giansanti et al., 2007; Robinett et al., 2009). However, while *gio*, *fwd* and *Rab11* mutant spermatocytes exhibit an abnormal accumulation of Lva-containing Golgi-derived vesicles at the telophase equator, spermatocytes from *fws* or *bru* mutant do not exhibit this effect. Those latter results led us to propose that *gio*, *fwd* and *Rab11* are required for membrane–vesicle fusion at the cleavage site, whereas *fws* and *bru* are not essential for this process (Giansanti et al., 2006; Giansanti et al., 2007; Robinett et al., 2009). Impairment of *zw10* or *rint1* function does not result in an accumulation of Lva-positive vesicles near the cleavage site, suggesting that these genes, like *fws* and *bru,* are not required for vesicle fusion with the equatorial membrane.

Zw10 binds the dynactin complex, suggesting that the Zw10 subunit of the RZZ complex helps recruit dynactin to the kinetochore, thereby mediating the dynein-dependent shedding of SAC proteins along the kinetochore MTs (Howell et al., 2001; Starr et al., 1998; Wojcik et al., 2001; Williams et al., 1996). In mammalian cells, ZW10 is thought to play a dynactin-binding role within both the RZZ and the NRZ complexes (Schmitt, 2010; Sun et al., 2007; Varma et al., 2006). The cytokinesis defect in *zw10* mutants might therefore simply reflect lack of dynactin binding to cytokinetic structures such as the central spindle or the Golgi-derived vesicles. Several observations suggest that this scenario is unlikely. First, the localization pattern of Zw10 in *Drosophila* male germ cells is quite different from that of the dynein heavy chain (Anderson et al., 2009) or the Dlic dynein light intermediate chain (also called Dlic2 or CG1938; see supplementary material Fig. S1). Dynein/dynactin is enriched at the nuclear membrane and around the centrosomes of spermatocytes, and forms a hemispherical cup on the side of the nucleus opposite to the acroblast in spermatids (Anderson et al., 2009). Second, mutations in *asunder* (*asun*), a gene required for proper dynein/dynactin localization in spermatocytes, do disrupt cytokinesis but cause a phenotype completely different from that of *zw10* mutants. In *asun* mutants, spermatocytes exhibit early defects in spindle assembly and do not appear to be able to form a central spindle (Anderson et al., 2009). Third, mutations in the *dynein light chain 1* gene (*ddlc1,* also called *ctp* or *CG6998*) disrupt several aspects of spermatid growth but fail to affect cytokinesis (Ghosh-Roy et al., 2004). Together, these data suggest that disruption of cytokinesis in *zw10* mutants is not due to abnormal dynein/dynactin behavior but is rather a consequence of a dynein-independent defect in membrane trafficking.

A different alternative is that the cytokinesis defects elicited by loss of Zw10 or Rint1 are due to problems in Golgi behaviour during meiosis. It has previously been reported that certain proteins enriched in the interphase Golgi stacks and required for cytokinesis must properly dissociate from the Golgi to fulfill their cytokinetic role. For example, if the Nir2 protein is not phosphorylated by Cdk1, it fails both to dissociate from the Golgi membranes and to interact with Plk1, leading to cytokinesis failures in HeLa cells (Litvak et al., 2004). Lva staining showed that aberrant Golgi stacks of Zw10- and Rint1-depleted spermatocytes break down into fragments during meiotic division, just as their wild-type counterparts (Fig. 6E; supplementary material Fig. S4E). It thus appears that problems in Golgi breakdown cannot explain the cytokinesis defects caused by Zw10 or Rint1 loss. Our current working model is that Zw10 and Rint1 control features of the ER–Golgi trafficking that are essential for correct formation and/or composition of the vesicles required for membrane expansion during cytokinesis. These features might include maintenance of the correct Golgi structure and/or proper release of membrane traffic proteins from Golgi membranes.

The role of the spindle envelope in *Drosophila* male meiosis

We have shown that in dividing spermatocytes Zw10, Rod and Zwilch all accumulate at the spindle envelope midzone (SEMZ); a similar enrichment at the SEMZ was previously observed for Mast/Orbit, Cenp-Meta and NudE (Inoue et al., 2004; Wainman et al., 2009). However, when the RZZ complex fails to form, none of its components accumulate at the SEMZ. The localization of Zw10 at the SEMZ can therefore not be essential for cytokinesis, because *zwilch* and *rod* mutants lacking the Zw10 band at the SEMZ are not cytokinesis defective. Although Zw10, Rod, Zwilch, Mast/Orbit, Cenp-Meta and NudE have different functions in cell division (Inoue et al., 2004; Karess, 2005; Wainman et al., 2009), they share the property of being enriched at both the kinetochores and the SEMZ. This fact raises the possibility that most *Drosophila* proteins that accumulate at the kinetochore, but are not integral components of this structure, move to the SEMZ and concentrate there during spermatocyte ana-telophase.

What is the biological meaning of the localization of Zw10, Rod, Zwilch, Cenp-Meta and NudE at the SEMZ? A possible answer is suggested by studies on the mammalian homologues of these proteins. ZW10, NUDE/NUDEL and CENP-E (the Cenp-Meta homologue) localize to the midbody, even if none of these proteins is directly required for cytokinesis (Brown et al., 1994; Feng and Walsh, 2004; Scaërou et al., 2001; Stehman et al., 2007; Williams et al., 1996). Interestingly, CENP-E is specifically degraded at the end of cell division (Brown et al., 1994), and failure to degrade CENP-E due to loss of the ubiquitin ligase component Skp1 causes cytokinesis defects (Liu et al., 2006). These results raise the possibility that targeting of Zw10, Rod, Zwilch, Mast/Orbit, Cenp-Meta and NudE to the SEMZ (and eventually to the midbody) might facilitate their degradation via the ubiquitin–proteasome pathway. Consistent with this possibility, several factors involved in this degradation pathway localize to the midbody, and several proteins required for cytokinesis such as Plk1 and survivin are degraded at this site during the final phase of the process (Pohl and Jentsch, 2008 and references therein).

Spermatocyte cytokinesis is particularly dependent on membrane trafficking

Zw10 is required for meiotic cytokinesis in males but not for mitotic cytokinesis, as mutant larval brains exhibit many aneuploid metaphases but no polyploid cells (Smith et al., 1985; Williams et al., 1992; Williams et al., 1996). Previous studies have shown that null mutations in *fwd* (PI4Kβ), *fws* (Cog5) and *bru* (TRAPPII) disrupt spermatocyte cytokinesis but have no observable effects on larval neuroblast mitosis (Brill et al., 2000; Farkas et al., 2003; Giansanti et al., 2004; Robinett et al., 2009). Similarly, null mutations in *gio* (PITP) and *Arf6* cause very mild defects in somatic cell cytokinesis (both exhibit ~5% polyploid cells in mutant brains) but completely disrupt spermatocyte cytokinesis (both exhibit >90% multinucleated spermatids) (Dyer et al., 2007; Gatt and Glover, 2006; Giansanti et al., 2006). Finally, hypomorphic mutations in *Rab11* block male meiotic cytokinesis but do not affect larval neuroblast mitosis (Giansanti et al., 2007). In summary, all membrane traffic mutants so far characterized are severely defective in spermatocyte cytokinesis but not in larval neuroblast cytokinesis. Dividing spermatocytes therefore appear to require a particularly efficient membrane addition process during cytokinesis.

The reason for this characteristic feature of *Drosophila* spermatocytes is currently unclear. One possibility is that the requirements of membrane trafficking functions for spermatocyte cytokinesis reflect the unusually complex organization of membrane stores within these cells, which include multiple Golgi stacks and the astral and parafusorial membranes of the ER (Tates, 1971) (see also Fig. 2A–C). Membrane formation during spermatocyte cytokinesis would thus require trafficking activities that are either unneeded or redundant in neuroblasts, which do not contain such large membrane stores. An alternative hypothesis, which we favor, is that spermatocytes have a very limited plasma membrane reservoir compared to somatic cells. Indeed, EM analysis has shown that spermatocytes lack plasma membrane protrusions and microvilli (Tates, 1971), whereas both neuroblasts and S2 cells display very large membrane protrusions near the cleavage site (Somma et al., 2002) (our unpublished observations). Thus, it is conceivable that in contrast to somatic cells, spermatocytes do not possess enough preexisting plasma membrane to be reorganized during cytokinesis and instead must rely on the membrane trafficking machinery to produce the new membrane required for furrow ingression.

Materials and Methods

Fly strains and genetic manipulations

All of the RZZ mutations used here are strong hypomorphs/nulls. We used $zw10^{65i20}$ and $zw10^{65l21}$ also called $mit(1)15^{4}$ and $mit(1)15^{5}$, respectively (FlyBase) (Shannon et al., 1972; Smith et al., 1985; Williams et al., 2003). We sequenced both mutant alleles and found that they both carry in-frame deletions; the $zw10^{65l21}$ deletion results in a protein lacking seven amino acids (aa; 362–368), while the deletion observed in $zw10^{65i20}$ produces *a* protein lacking 35 aa (362–368). $zw10^{65l21}$ was employed for immunofluorescence studies and is referenced as *zw10* in the text. The mutations $zwilch^{1229}$ (Williams et al., 2003), rod^{1100} (Savoian et al., 2000) were described previously. We sequenced the rod^{1100} mutant allele; it carries a G to A transition at position 2462 that creates a stop codon resulting in a truncated Rod protein of 820 aa (compared with the 2089 aa of wild-type Rod). The $nudE^{39E}$ and $cenp\text{-}meta^{A}$ mutant alleles are described by Wainman and colleagues (Wainman et al., 2009). The strain expressing ER–EYFP (LaJeunesse et al., 2004) was obtained from the Bloomington Stock Center. The strains expressing β-tubulin–EGFP (Inoue et al., 2004), Sqh–GFP (Royou et al., 2004), and Dlic–GFP were kindly provided by D. Glover, R. Karess and J. Raff, respectively. All flies were reared according to standard procedures at 25℃.

To knock down the *rint1* gene we used the v109761 VDRC (Vienna *Drosophila* RNAi Center) line carrying a *UAS-rint1*RNAi construct. We crossed v109761 males to females carrying the testis-specific *bam-GAL4* driver (Chen and McKearin, 2003); testes of F1 males were then examined for Golgi number and morphology, and cytokinesis defects.

Cytology and immunofluorescence

Cytological preparations were made from third instar larvae testes. For immunostaining with anti-Zw10 (Williams et al., 2003), anti-Zwilch (Williams et al., 2003), anti-Rod (Scaërou et al., 1999) or anti-p120 antibodies (Calbiochem, anti-*Drosophila* Golgi; no longer available) testes were fixed as described by Starr et al. (Starr et al., 1998). For immunostaining with other antibodies and for F-actin staining, testes were fixed according to Giansanti et al. and Gunsalus et al., respectively (Giansanti et al., 1999; Gunsalus et al., 1995). The following dilutions were used: mouse anti-α-tubulin (T 6199 Sigma, St Louis, MO) 1:500; mouse FITC-conjugated anti-α-tubulin (F 2168 Sigma; used for double Pnut and tubulin immunostaining); mouse anti-p120 (1:100); mouse anti-Peanut (1:3; Hybridoma bank, Iowa City, Iowa); rabbit anti-anillin (Field and Alberts, 1995) 1:1000; rabbit anti-Feo (Vernì et al., 2004) 1:200; rabbit anti-Lva (Sisson et al., 2000) 1:1000. Double staining with fluorescein-labeled WGA (Molecular Probes, Eugene, OR) and anti-Zw10, anti-Rod or anti-Zwilch antibodies was performed as described previously (Giansanti et al., 2006). Alexa Fluor 555 goat anti-rabbit (1:300; Invitrogen) and FITC- or Rhodamine-conjugated goat anti-mouse (1:20; Jackson ImmunoResearch) were used as secondary antibodies. All slides were mounted in Vectashield medium H-1200 with 4,6 diamidino-2-phenylindole (DAPI) (Vector Laboratories, Burlingame, CA) to stain DNA. Images were captured as described previously (Giansanti et al., 2006). Mature spermatocyte Golgi stacks stained for

Lva were imaged at 0.5 μm steps through the whole cell using an Olympus FV1000 confocal microscope.

Live imaging

To view male meiosis in vivo, testes were prepared as described by Inoue and colleagues (Inoue et al., 2004) and imaged as described by Giansanti and colleagues (Giansanti et al., 2007). Images were collected at 1-minute intervals and movies were created using the Metamorph software (Universal Imaging Corp.). Cell perimeters were measured using image J (NIH; http://rsbweb.nih.gov/ij/).

Acknowledgements

We thank K. Field, D. Glover, R. Karess, O. Papoulas, M. Savoian and J. Raff for generously providing *Drosophila* strains and antibodies.

Funding

A.W. was supported by a fellowship from a European Community Training and Mobility of Researchers grant [grant number HPRNCT-2002-00260 to M.G.]. Research was supported by the Program for Research of National Interest (PRIN) to M.G. and M.G.G.; the Italian Association for Cancer Research [grant numbers IG10775 to M.G.G. and IG10793 to M.G.]; and the National Institutes of Health [grant number GM048430 to M.L.G.]. Deposited in PMC for release after 12 months.

Supplementary material available online at
http://jcs.biologists.org/lookup/suppl/doi:10.1242/jcs.099820/-/DC1

References

Albertson, R., Riggs, B. and Sullivan, W. (2005). Membrane traffic: a driving force in cytokinesis. *Trends Cell Biol.* **15**, 92-101.

Anderson, M. A., Jodoin, J. N., Lee, E., Hales, K. G., Hays, T. S. and Lee, L. A. (2009). Asunder is a critical regulator of dynein-dynactin localization during Drosophila spermatogenesis. *Mol. Biol. Cell* **20**, 2709-2721.

Aoki, T., Ichimura, S., Itoh, A., Kuramoto, M., Shinkawa, T., Isobe, T. and Tagaya, M. (2009). Identification of the neuroblastoma-amplified gene product as a component of the syntaxin 18 complex implicated in Golgi-to-endoplasmic reticulum retrograde transport. *Mol. Biol. Cell* **20**, 2639-2649.

Arasaki, K., Taniguchi, M., Tani, K. and Tagaya, M. (2006). RINT-1 regulates the localization and entry of ZW10 to the syntaxin 18 complex. *Mol. Biol. Cell* **17**, 2780-2788.

Arasaki, K., Uemura, T., Tani, K. and Tagaya, M. (2007). Correlation of Golgi localization of ZW10 and centrosomal accumulation of dynactin. *Biochem. Biophys. Res. Commun.* **359**, 811-816.

Bobinnec, Y., Marcaillou, C., Morin, X. and Debec, A. (2003). Dynamics of the endoplasmic reticulum during early development of Drosophila melanogaster. *Cell Motil. Cytoskeleton* **54**, 217-225.

Brill, J. A., Hime, G. R., Scharer-Schuksz, M. and Fuller, M. T. (2000). A phospholipid kinase regulates actin organization and intercellular bridge formation during germline cytokinesis. *Development* **127**, 3855-3864.

Brown, K. D., Coulson, R. M., Yen, T. J. and Cleveland, D. W. (1994). Cyclin-like accumulation and loss of the putative kinetochore motor CENP-E results from coupling continuous synthesis with specific degradation at the end of mitosis. *J. Cell Biol.* **125**, 1303-1312.

Cenci, G., Bonaccorsi, S., Pisano, C., Verni, F. and Gatti, M. (1994). Chromatin and microtubule organization during premeiotic, meiotic and early postmeiotic stages of Drosophila melanogaster spermatogenesis. *J. Cell Sci.* **107**, 3521-3534.

Chen, D. and McKearin, D. M. (2003). A discrete transcriptional silencer in the bam gene determines asymmetric division of the Drosophila germline stem cell. *Development* **130**, 1159-1170.

Civril, F., Wehenkel, A., Giorgi, F. M., Santaguida, S., Di Fonzo, A., Grigorean, G., Ciccarelli, F. D. and Musacchio, A. (2010). Structural analysis of the RZZ complex reveals common ancestry with multisubunit vesicle tethering machinery. *Structure* **18**, 616-626.

D'Avino, P. P. (2009). How to scaffold the contractile ring for a safe cytokinesis – lessons from Anillin-related proteins. *J. Cell Sci.* **122**, 1071-1079.

D'Avino, P. P., Savoian, M. S. and Glover, D. M. (2005). Cleavage furrow formation and ingression during animal cytokinesis: a microtubule legacy. *J. Cell Sci.* **118**, 1549-1558.

Dyer, N., Rebollo, E., Domínguez, P., Elkhatib, N., Chavrier, P., Daviet, L., González, C. and González-Gaitán, M. (2007). Spermatocyte cytokinesis requires rapid membrane addition mediated by ARF6 on central spindle recycling endosomes. *Development* **134**, 4437-4447.

Eggert, U. S., Mitchison, T. J. and Field, C. M. (2006). Animal cytokinesis: from parts list to mechanisms. *Annu. Rev. Biochem.* **75**, 543-566.

Farkas, R. M., Giansanti, M. G., Gatti, M. and Fuller, M. T. (2003). The Drosophila Cog5 homologue is required for cytokinesis, cell elongation, and assembly of specialized Golgi architecture during spermatogenesis. *Mol. Biol. Cell* **14**, 190-200.

Feng, Y. and Walsh, C. A. (2004). Mitotic spindle regulation by Nde1 controls cerebral cortical size. *Neuron* **44**, 279-293.

Field, C. M. and Alberts, B. M. (1995). Anillin, a contractile ring protein that cycles from the nucleus to the cell cortex. *J. Cell Biol.* **131**, 165-178.

Fuller, M. T. (1993). Spermatogenesis. In *The Development of Drosophila melanogaster*, vol. 1 (ed. M. Bate and A. Martinez-Arias), pp. 71-146. Cold Spring Harbo, NY: Laboratory Press.

Gatt, M. K. and Glover, D. M. (2006). The Drosophila phosphatidylinositol transfer protein encoded by vibrator is essential to maintain cleavage-furrow ingression in cytokinesis. *J. Cell Sci.* **119**, 2225-2235.

Ghosh-Roy, A., Kulkarni, M., Kumar, V., Shirolikar, S. and Ray, K. (2004). Cytoplasmic dynein-dynactin complex is required for spermatid growth but not axoneme assembly in Drosophila. *Mol. Biol. Cell* **15**, 2470-2483.

Giansanti, M. G., Bonaccorsi, S., Williams, B., Williams, E. V., Santolamazza, C., Goldberg, M. L. and Gatti, M. (1998). Cooperative interactions between the central spindle and the contractile ring during Drosophila cytokinesis. *Genes Dev.* **12**, 396-410.

Giansanti, M. G., Bonaccorsi, S. and Gatti, M. (1999). The role of anillin in meiotic cytokinesis of Drosophila males. *J. Cell Sci.* **112**, 2323-2334.

Giansanti, M. G., Farkas, R. M., Bonaccorsi, S., Lindsley, D. L., Wakimoto, B. T., Fuller, M. T. and Gatti, M. (2004). Genetic dissection of meiotic cytokinesis in Drosophila males. *Mol. Biol. Cell* **15**, 2509-2522.

Giansanti, M. G., Bonaccorsi, S., Kurek, R., Farkas, R. M., Dimitri, P., Fuller, M. T. and Gatti, M. (2006). The class I PITP giotto is required for Drosophila cytokinesis. *Curr. Biol.* **16**, 195-201.

Giansanti, M. G., Belloni, G. and Gatti, M. (2007). Rab11 is required for membrane trafficking and actomyosin ring constriction in meiotic cytokinesis of Drosophila males. *Mol. Biol. Cell* **18**, 5034-5047.

González, C., Casal, J. and Ripoll, P. (1989). Relationship between chromosome content and nuclear diameter in early spermatids of Drosophila melanogaster. *Genet. Res.* **54**, 205-212.

Gunsalus, K. C., Bonaccorsi, S., Williams, E., Verni, F., Gatti, M. and Goldberg, M. L. (1995). Mutations in twinstar, a Drosophila gene encoding a cofilin/ADF homologue, result in defects in centrosome migration and cytokinesis. *J. Cell Biol.* **131**, 1243-1259.

Hirose, H., Arasaki, K., Dohmae, N., Takio, K., Hatsuzawa, K., Nagahama, M., Tani, K., Yamamoto, A., Tohyama, M. and Tagaya, M. (2004). Implication of ZW10 in membrane trafficking between the endoplasmic reticulum and Golgi. *EMBO J.* **23**, 1267-1278.

Howell, B. J., McEwen, B. F., Canman, J. C., Hoffman, D. B., Farrar, E. M., Rieder, C. L. and Salmon, E. D. (2001). Cytoplasmic dynein/dynactin drives kinetochore protein transport to the spindle poles and has a role in mitotic spindle checkpoint inactivation. *J. Cell Biol.* **155**, 1159-1172.

Inoue, M., Arasaki, K., Ueda, A., Aoki, T. and Tagaya, M. (2008). N-terminal region of ZW10 serves not only as a determinant for localization but also as a link with dynein function. *Genes Cells* **13**, 905-914.

Inoue, Y. H., Savoian, M. S., Suzuki, T., Máthé, E., Yamamoto, M. T. and Glover, D. M. (2004). Mutations in orbit/mast reveal that the central spindle is comprised of two microtubule populations, those that initiate cleavage and those that propagate furrow ingression. *J. Cell Biol.* **166**, 49-60.

Karess, R. (2005). Rod-Zw10-Zwilch: a key player in the spindle checkpoint. *Trends Cell Biol.* **15**, 386-392.

Kondylis, V. and Rabouille, C. (2009). The Golgi apparatus: lessons from Drosophila. *FEBS Lett.* **583**, 3827-3838.

LaJeunesse, D. R., Buckner, S. M., Lake, J., Na, C., Pirt, A. and Fromson, K. (2004). Three new Drosophila markers of intracellular membranes. *Biotechniques* **36**, 784-790.

Litvak, V., Argov, R., Dahan, N., Ramachandran, S., Amarilio, R., Shainskaya, A. and Lev, S. (2004). Mitotic phosphorylation of the peripheral Golgi protein Nir2 by Cdk1 provides a docking mechanism for Plk1 and affects cytokinesis completion. *Mol. Cell* **14**, 319-330.

Liu, D., Zhang, N., Du, J., Cai, X., Zhu, M., Jin, C., Dou, Z., Feng, C., Yang, Y., Liu, L. et al. (2006). Interaction of Skp1 with CENP-E at the midbody is essential for cytokinesis. *Biochem. Biophys. Res. Commun.* **345**, 394-402.

McKay, H. F. and Burgess, D. R. (2011). 'Life is a highway': membrane trafficking during cytokinesis. *Traffic* **12**, 247-251.

Montagnac, G., Echard, A. and Chavrier, P. (2008). Endocytic traffic in animal cell cytokinesis. *Curr. Opin. Cell Biol.* **20**, 454-461.

Musacchio, A. and Salmon, E. D. (2007). The spindle-assembly checkpoint in space and time. *Nat. Rev. Mol. Cell Biol.* **8**, 379-393.

Neufeld, T. P. and Rubin, G. M. (1994). The Drosophila peanut gene is required for cytokinesis and encodes a protein similar to yeast putative bud neck filament proteins. *Cell* **77**, 371-379.

Pohl, C. and Jentsch, S. (2008). Final stages of cytokinesis and midbody ring formation are controlled by BRUCE. *Cell* **132**, 832-845.

Polevoy, G., Wei, H. C., Wong, R., Szentpetery, Z., Kim, Y. J., Goldbach, P., Steinbach, S. K., Balla, T. and Brill, J. A. (2009). Dual roles for the Drosophila PI 4-kinase four wheel drive in localizing Rab11 during cytokinesis. *J. Cell Biol.* **187**, 847-858.

Prekeris, R. and Gould, G. W. (2008). Breaking up is hard to do – membrane traffic in cytokinesis. *J. Cell Sci.* **121**, 1569-1576.

Robinett, C. C., Giansanti, M. G., Gatti, M. and Fuller, M. T. (2009). TRAPPII is required for cleavage furrow ingression and localization of Rab11 in dividing male meiotic cells of Drosophila. *J. Cell Sci.* **122**, 4526-4534.

Royou, A., Field, C., Sisson, J. C., Sullivan, W. and Karess, R. (2004). Reassessing the role and dynamics of nonmuscle myosin II during furrow formation in early Drosophila embryos. *Mol. Biol. Cell* **15**, 838-850.

Savoian, M. S., Goldberg, M. L., and Rieder, C. L. (2000). The rate of poleward chromosome motion is attenuated in Drosophila zw10 and rod mutants. *Nat. Cell Biol.* **2**, 948-952.

Scaërou, F., Aguilera, I., Saunders, R., Kane, N., Blottière, L. and Karess, R. (1999). The rough deal protein is a new kinetochore component required for accurate chromosome segregation in Drosophila. *J. Cell Sci.* **112**, 3757-3768.

Scaërou, F., Starr, D. A., Piano, F., Papoulas, O., Karess, R. E. and Goldberg, M. L. (2001). The ZW10 and Rough Deal checkpoint proteins function together in a large, evolutionarily conserved complex targeted to the kinetochore. *J. Cell Sci.* **114**, 3103-3114.

Schmitt, H. D. (2010). Dsl1p/Zw10: common mechanisms behind tethering vesicles and microtubules. *Trends Cell Biol.* **20**, 257-268.

Shannon, M. P., Kaufman, T. C., Shen, M. W. and Judd, B. H. (1972). Lethality patterns and morphology of selected lethal and semi-lethal mutations in the zeste-white region of Drosophila melanogaster. *Genetics* **72**, 615-638.

Sisson, J. C., Field, C., Ventura, R., Royou, A. and Sullivan, W. (2000). Lava lamp, a novel peripheral golgi protein, is required for Drosophila melanogaster cellularization. *J. Cell Biol.* **151**, 905-918.

Smith, D. A., Baker, B. S. and Gatti, M. (1985). Mutations in genes encoding essential mitotic functions in Drosophila melanogaster. *Genetics* **110**, 647-670.

Somma, M. P., Fasulo, B., Cenci, G., Cundari, E. and Gatti, M. (2002). Molecular dissection of cytokinesis by RNA interference in Drosophila cultured cells. *Mol. Biol. Cell* **13**, 2448-2460.

Stanley, H., Botas, J. and Malhotra, V. (1997). The mechanism of Golgi segregation during mitosis is cell type-specific. *Proc. Natl. Acad. Sci. USA* **94**, 14467-14470.

Starr, D. A., Williams, B. C., Hays, T. S. and Goldberg, M. L. (1998). ZW10 helps recruit dynactin and dynein to the kinetochore. *J. Cell Biol.* **142**, 763-774.

Stehman, S. A., Chen, Y., McKenney, R. J. and Vallee, R. B. (2007). NudE and NudEL are required for mitotic progression and are involved in dynein recruitment to kinetochores. *J. Cell Biol.* **178**, 583-594.

Sun, Y., Shestakova, A., Hunt, L., Sehgal, S., Lupashin, V. and Storrie, B. (2007). Rab6 regulates both ZW10/RINT-1 and conserved oligomeric Golgi complex-dependent Golgi trafficking and homeostasis. *Mol. Biol. Cell* **18**, 4129-4142.

Tates, A. D. (1971). Cytodifferentiation during spermatogenesis in Drosophila melanogaster: an electron microscope study. PhD. Leiden: Rijksuniversiteit de Leiden.

Vallee, R. B., Varma, D. and Dujardin, D. L. (2006). ZW10 function in mitotic checkpoint control, dynein targeting and membrane trafficking: is dynein the unifying theme? *Cell Cycle* **5**, 2447-2451.

Varma, D., Dujardin, D. L., Stehman, S. A. and Vallee, R. B. (2006). Role of the kinetochore/cell cycle checkpoint protein ZW10 in interphase cytoplasmic dynein function. *J. Cell Biol.* **172**, 655-662.

Vernì, F., Somma, M. P., Gunsalus, K. C., Bonaccorsi, S., Belloni, G., Goldberg, M. L. and Gatti, M. (2004). Feo, the Drosophila homolog of PRC1, is required for central-spindle formation and cytokinesis. *Curr. Biol.* **14**, 1569-1575.

Wainman, A., Creque, J., Williams, B., Williams, E. V., Bonaccorsi, S., Gatti, M. and Goldberg, M. L. (2009). Roles of the Drosophila NudE protein in kinetochore function and centrosome migration. *J. Cell Sci.* **122**, 1747-1758.

Williams, B. C. and Goldberg, M. L. (1994). Determinants of Drosophila zw10 protein localization and function. *J. Cell Sci.* **107**, 785-798.

Williams, B. C., Karr, T. L., Montgomery, J. M. and Goldberg, M. L. (1992). The Drosophila l(1)zw10 gene product, required for accurate mitotic chromosome segregation, is redistributed at anaphase onset. *J. Cell Biol.* **118**, 759-773.

Williams, B. C., Gatti, M. and Goldberg, M. L. (1996). Bipolar spindle attachments affect redistributions of ZW10, a Drosophila centromere/kinetochore component required for accurate chromosome segregation. *J. Cell Biol.* **134**, 1127-1140.

Williams, B. C., Li, Z., Liu, S., Williams, E. V., Leung, G., Yen, T. J. and Goldberg, M. L. (2003). Zwilch, a new component of the ZW10/ROD complex required for kinetochore functions. *Mol. Biol. Cell* **14**, 1379-1391.

Wilson, K. L., Fitch, K. R., Bafus, B. T. and Wakimoto, B. T. (2006). Sperm plasma membrane breakdown during Drosophila fertilization requires sneaky, an acrosomal membrane protein. *Development* **133**, 4871-4879.

Wojcik, E., Basto, R., Serr, M., Scaërou, F., Karess, R. and Hays, T. (2001). Kinetochore dynein: its dynamics and role in the transport of the Rough deal checkpoint protein. *Nat. Cell Biol.* **3**, 1001-1007.

Xu, H., Brill, J. A., Hsien, J., McBride, R., Boulianne, G. L. and Trimble, W. S. (2002). Syntaxin 5 is required for cytokinesis and spermatid differentiation in Drosophila. *Dev. Biol.* **251**, 294-306.

Journal of Cell Science